Development of Non-Invasive Acoustic Sensing-Based Framework for Early Detection of Red Palm Weevil Larval Activity

S. E. Zahedi[1], M. Aboonajmi[1*], S. R. Hassan Beygi Bidgoli[1]

1- Department of Agrotechnology, College of Abouraihan, University of Tehran, Iran
(*- Corresponding Author Email: abonajmi@ut.ac.ir)
https://doi.org/10.22067/jam.2026.96621.1447

Abstract

The red palm weevil (*Rhynchophorus ferrugineus*) is a destructive pest of date palms whose concealed larval feeding makes early detection extremely difficult. To capture weak chewing signals under natural orchard conditions, a portable bioacoustic sensing unit was developed using a MAX9814 electret microphone integrated with an STM32F103C8T6 12-bit data acquisition module operating at 16 kHz. The compact design, isolated power, and vibration-damping mount enabled reliable, non-invasive recording in field conditions. Acoustic emissions from infested palms were analysed in both time and frequency domains using six key spectral features: mean and median frequency, band power, occupied and power bandwidth, and peak location, across five frame durations. Statistical analysis revealed how segmentation scale affects signal stability, impulsiveness, and redundancy among features. A structured spectral atlas was then established, consolidating scattered acoustic descriptors into a unified representation. Dominant larval activity occurred below 7 kHz, with mean and median frequencies between 2.1 and 3.8 kHz ($r > 0.85$), and Band power values ranged from approximately 1.7×10^{-5} to 2.6×10^{-5} (relative linear scale) and increased during periods of intense chewing. The occupied bandwidth (1.5 to 2.8 kHz) narrowed during intense chewing, confirming spectral consistency and diagnostic value. Unlike prior studies that primarily report classification performance, this work introduces a structured spectral atlas that quantitatively characterises the stability, variability, and interrelationships of key acoustic features across multiple time scales. This descriptive baseline provides a foundation for informed feature selection, sensor bandwidth design, and the development of future embedded, non-invasive acoustic systems for early RPW infestation monitoring.

Keywords: Bioacoustic sensing, Date palm, Early detection, Red palm weevil, Spectral features

Introduction

The red palm weevil (*Rhynchophorus ferrugineus*, RPW) is recognised as one of the most economically devastating pests affecting Phoenix dactylifera cultivation across the Middle East, North Africa, and Southeast Asia. During the larval stage, the insect burrows into the date palm trunk and consumes internal tissues, leading to severe structural degradation that often precedes visible symptoms (Hoddle *et al.*, 2024; Siddiqui *et al.*, 2025). The concealed nature of infestation substantially reduces the efficacy of conventional detection techniques, such as visual inspection or mechanical probing, which rarely identify early-stage activity (Faleiro, 2006). Fig. 1 shows a date palm that has collapsed due to late detection of RPW infestation, illustrating the extensive internal damage caused by larval feeding.

Fig. 1. The date palm trunk collapsed as a result of severe internal damage from late-stage red palm weevil infestation

Over the past decade, acoustic signal processing has emerged as a valuable approach for detecting subtle biological and mechanical phenomena in agricultural systems. A growing number of studies have shown the effectiveness of time-domain and frequency-domain analyses in monitoring structural conditions and biological activity. For example, acoustic signatures have been used to detect faults in agricultural gearboxes (Zamani, Aboonajmi, & Hassan-Beygi, 2016), characterise impulse responses in melon varieties (Khoshnam, Bidgoly, Namjoo, & Doroozi, 2017), and assess vocal signals for poultry maturity diagnosis (Yavari, Banakar, & Sharafi, 2020). Other research has examined signal complexity using fractal dimensions in combine harvesters (Broujeni & Maleki, 2017) and investigated soil texture through acoustic feedback from cone penetrometers (Nasrollahi Azar, Farrokhi Teimourlou, & Rostampour, 2023). These applications collectively demonstrate how acoustic sensing can be harnessed for practical diagnostics in agriculture, especially when dealing with non-stationary, low-amplitude signals.

Within this broader context, the use of bioacoustics for pest detection has gained increasing attention. Bioacoustic monitoring of the red palm weevil offers a non-invasive strategy for detecting internal larval activity before visual symptoms appear (Delalieux *et al.*, 2023; Mendel, Voet, Nazarian, Dobrinin, & Ment, 2024). The underlying principle involves capturing broadband, impulsive sound signals generated by larval chewing and movement using embedded sensors, followed by detailed signal processing (Torky, Dahy, & Hassanien, 2023). Previous research has identified key acoustic features—such as roll-off, entropy, and dominant frequency content—that differentiate pest-generated signals from environmental noise. (Mankin, Hagstrum, Smith, Roda, & Kairo, 2011; Rach *et al.*, 2013).

Despite the growing body of work on acoustic detection of red palm weevil infestation, most existing studies emphasise classification accuracy or sensor feasibility, while providing limited insight into the underlying structure and stability of the acoustic features themselves. Spectral descriptors are often employed as isolated inputs to detection models, with little analysis of their distributional behaviour, temporal consistency, or inter-feature relationships across different segmentation scales. This limits interpretability and complicates the translation of reported performance into robust sensor design and feature selection.

In response to this gap, the present study introduces a structured spectral atlas that systematically characterises key frequency-domain features across multiple time-window durations. By focusing on descriptive statistics and feature relationships rather than detection performance, the proposed framework provides a biologically grounded reference that complements existing approaches and supports future development of non-invasive acoustic monitoring systems.

Previous studies have mainly focused on building classification models to distinguish infested palms from healthy ones, but they often overlooked the detailed structure of the acoustic signals themselves. This research addresses that gap by developing a spectral atlas that describes how key acoustic features such as mean frequency, median frequency, and bandwidth, change over time. Instead of creating another detection algorithm, the study provides a descriptive and quantitative understanding of the signal's internal dynamics. This framework establishes a reliable baseline for future signal modelling, feature selection, and the design of embedded sensors optimised for the subtle bioacoustic patterns of red palm weevil larvae.

Materials and Methods

Bioacoustic recording system and signal acquisition

Acoustic recordings were conducted in open-field orchard conditions within a date palm plantation naturally exposed to environmental factors, including wind, insects, and distant agricultural activities. To preserve the authenticity of the soundscape while maintaining data integrity, recordings were taken during calm periods when transient or non-representative noises—such as short bursts from farm machinery or nearby mechanical tools—were absent. This ensured that the captured waveforms reflected the ordinary acoustic background of palm cultivation rather than sporadic artificial disturbances.

A MAX9814 electret condenser microphone module (Adafruit Industries LLC, New York, NY, USA) served as the primary acoustic sensor. The module integrates a low-noise preamplifier, an automatic gain control (AGC) circuit, and bias circuitry in a compact board, which collectively enhance signal detectability under field conditions. The integrated AGC dynamically adapts the gain based on input level, preventing saturation when unexpected transient sounds occur and maintaining sensitivity to low-amplitude larval chewing signals. The module provides three selectable fixed gains namely 40, 50, and 60 dB, allowing adaptability to different wood densities and environmental noise levels. A gain of 50 dB was selected as it provided sufficient amplitude margin for low-intensity biological emissions without amplifying background noise excessively. The unit's wide frequency response ensures coverage of the entire acoustic band in which Red Palm Weevil (RPW) larval activity occurs.

The analogue output of the microphone was digitised using an STM32F103C8T6 microcontroller (STMicroelectronics, Geneva, Switzerland), which integrates a 12-bit successive-approximation analogue-to-digital converter (ADC) with up to one mega sample per second throughput. Sampling was configured at 16 kHz, a rate that provides high temporal resolution while maintaining manageable data volume for field deployment. Continuous data streaming was achieved through Direct Memory Access (DMA), allowing the ADC to transfer samples directly into dual memory buffers without CPU interruption. This architecture prevents buffer underflow and guarantees gap-free acquisition. The ARM Cortex-M3 core operates at 72 MHz, ensuring deterministic timing and low-jitter conversion, critical for the short impulsive events typical of larval chewing.

The entire system was assembled as a portable field unit, consisting of the microphone probe, the microcontroller and SD-card data logger, a small display interface for monitoring operation, and detachable power storage. This configuration allowed efficient relocation among sampling trees and reduced setup time, an important consideration for outdoor measurements. The design ensured that data could be acquired continuously over long durations without requiring external computers or high-power infrastructure.

Field recordings were obtained from mature *Phoenix dactylifera* palms in Jahrom, Iran. Both infested and healthy trees were included. Infestation status was verified by agricultural specialists based on visible indicators such as sap exudation, frass accumulation, or perforation holes. Selected trees were of comparable age, trunk diameter, and canopy structure to minimise variability unrelated to infestation. Concurrent environmental parameters including air temperature, relative humidity, and ambient background noise were recorded to contextualise each dataset, as these factors influence larval activity and acoustic propagation through palm tissue; temperature and humidity were measured using a portable digital thermo-hygrometer (Model HD-3008, Lutron Electronic Enterprise Co., Ltd., Taipei, Taiwan), based on a thin-film capacitance humidity sensor and integrated temperature probe, with a measurement resolution of 0.1% RH and 0.1 °C. Acoustic data were collected in situ from standing date palm trees without physical sampling, cutting, or laboratory preparation. Both infested and non-infested palms were selected. Infestation status was determined a priori by agricultural specialists based on established field indicators, including sap exudation, frass accumulation, tissue softening, or visible entry holes. Healthy trees were chosen from the same orchard and matched as closely as possible in age, trunk diameter, and canopy condition to reduce structural variability.

Recordings were obtained on intact trunk surfaces using a non-invasive contact-based sensing approach. No material removal or surface treatment was performed, ensuring that the recorded signals reflect natural internal activity under realistic orchard conditions.

This data acquisition system was designed according to biosystems-instrumentation principles, emphasising stable mechanical coupling to the biological medium, electrical integrity of the sensor–recorder interface, and traceable documentation of environmental context. Such integration of biological and engineering considerations ensures that the acquired acoustic signals are both representative of real orchard conditions and suitable for quantitative interpretation of red palm weevil activity. For acoustic acquisition, the microphone probe was placed in direct contact with the palm trunk using a standardised, non-invasive mounting procedure. A thin, compliant coupling layer was applied between the sensor housing and the trunk surface to minimise air gaps and improve vibrational transmission, and the probe was stabilised using a clamp-based fixture to reduce motion due to wind or handling. Recordings were conducted at comparable trunk heights (approximately 1.0-1.2 m above ground level) on intact surface sections, with consistent sensor orientation and contact conditions across all trees. Although minor variability in coupling and tissue properties is unavoidable under field conditions, the use of a uniform attachment protocol ensured that the observed spectral patterns predominantly reflect internal acoustic activity rather than sensor placement artefacts, consistent with realistic non-invasive deployment scenarios. Fig. 2 illustrates the field-deployed bioacoustic setup installed on an infested date palm trunk in Jahrom, Iran, demonstrating the sensor arrangement and protective housing used during data collection.

Fig. 2. Field-deployed acoustic sensing system showing the protective housing and microphone setup on an infested date palm trunk.

The selection of the MAX9814 module is justified by its proven efficacy in prior bioacoustic research for capturing low-amplitude insect signals and internal plant vibrations, especially under conditions of solid mechanical coupling (Jeng, Yang, & Lee, 2011; Rach *et al.*, 2013). A key advantage of this microphone is its integrated Automatic Gain Control (AGC), which dynamically adjusts to amplitude fluctuations. This feature is crucial for faithfully recording the diverse acoustic profile of larval activity, which ranges from high-energy, impulsive chewing events to sustained, low-energy movements. Its compact form factor, low power requirements, and broad sensitivity bandwidth make it well-suited for embedded bioacoustic sensing applications in field conditions. Fig.3 illustrates the schematic configuration of the bioacoustic recording and signal acquisition system.

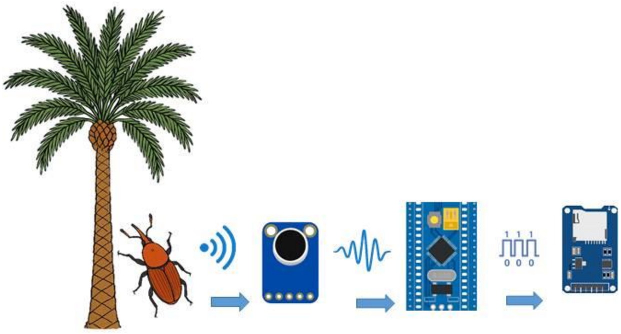

Fig. 3. Schematic configuration of the bioacoustic recording and signal acquisition system

Frequency-domain features

Larval chewing sounds contain rich information about behavioural states and interactions with substrate material. To capture these nuances, it is essential to characterise key spectral aspects of the acoustic signals, such as energy concentration, spectral spread, and dominant frequency content. Together, these spectral features enable a compact but meaningful representation of larval chewing acoustics.

- **Mean Frequency**: Represents the average frequency of the power spectrum, weighted by spectral amplitude. It reflects the overall spectral balance of the signal and can indicate shifts in dominant frequency content due to variations in chewing pressure, substrate density, or mandibular dynamics (Tzanetakis & Cook, 2002).
- **Median Frequency:** The frequency that divides the power spectrum into two halves. Unlike mean frequency, it is less sensitive to extreme values or noise. Median frequency provides a robust estimate of central tendency and helps differentiate between low-frequency-dominated versus high-frequency-dominated events.
- **Band Power:** Measures the total spectral energy within a specified frequency range. Higher band power typically corresponds to stronger or more forceful chewing events. It can also reflect changes in material resistance or larval activity intensity (Boashash, 2015).
- **Occupied Bandwidth:** The range of frequencies that contains a specified percentage (typically 99%) of the total spectral energy. This feature captures how concentrated or dispersed the acoustic energy is, offering insights into signal complexity and variability across chewing events.
- **Power Bandwidth:** The width of the spectrum above a defined power threshold, providing a measure of how broadly the energy is distributed across frequencies. A narrow power bandwidth may suggest tonal, structured emissions, while a wider spread indicates more broadband, noise-like behaviours (Dubnov, 2004).
- **Peak Location:** The frequency at which the maximum spectral amplitude occurs. This peak often corresponds to resonant

modes of chewing or vibrational responses of the substrate. Monitoring peak location helps identify dominant motion frequencies and potential biomechanical markers (Lartillot & Toiviainen, 2007).

By extracting spectral features frame-wise, we enable detailed temporal analysis that supports both supervised and unsupervised classification of larval behaviours. These features capture crucial signal characteristics such as dominant frequency content, spectral spread, and energy concentration, providing a compact yet informative representation of larval chewing acoustics. The features were extracted using MATLAB's signal Frequency Feature Extractor object, ensuring robust and consistent computation across recordings (Torky *et al.*, 2023).

Descriptive and statistical analysis of spectral features

To explore the acoustic characteristics of Red Palm Weevil larval activity, each frequency-domain feature was systematically evaluated using descriptive and statistical methodologies. In this study, spectral features including mean frequency, median frequency, band power, occupied bandwidth, power bandwidth, and peak location were analysed across recordings segmented at various temporal resolutions (0.2, 0.4, 0.6, 0.8, and 1.0 s).

To facilitate an exploratory analysis of larval acoustic behaviour, we computed a suite of distributional metrics for each spectral feature. Given the non-Gaussian and often impulsive nature of bioacoustic signals, the median and interquartile range (IQR) were employed as robust measures of central tendency and dispersion, respectively. The mean and standard deviation were also calculated for complementary reference, despite their sensitivity to outliers. Additional metrics, including skewness and kurtosis, were used to quantify distribution asymmetry and tail heaviness, providing critical insights into the prevalence of transient, high-energy chewing events. The interquartile range (IQR) was prioritised as a non-parametric measure of dispersion, effectively capturing the spread of the central 50% of data without relying on assumptions of normality. Additional statistics, including standard deviation**,** minimum**,** and maximum**,** were computed to provide a fuller descriptive picture of signal variation. To assess distribution shape, skewness quantifies asymmetry, while kurtosis characterises tail heaviness, both useful in identifying rare or impulsive acoustic phenomena associated with larval chewing activity.

These analyses aimed to reveal which descriptors remained stable or fluctuated across window durations, and to determine if larval feeding patterns produced skewed or heavy-tailed distributions, indicating impulsive activity. Understanding these patterns is essential for selecting reliable features in subsequent model development (Croarkin & Tobias, 2003).

Finally, we calculated Spearman's rank correlation between all feature pairs to assess monotonic relationships and potential redundancies. Spearman correlation is well-suited to bioacoustic data due to its robustness against non-normality and outliers (Conover, 1999). Correlation matrices were employed to detect highly interdependent features which inform decisions for dimensionality reduction and feature selection while preserving biological relevance.

Statistical analyses were conducted using MATLAB 2023a and Minitab 24 to inspect feature distributions, identify outliers, and qualitatively assess shifts in variability across different time resolutions. This approach aligns with best practices in exploratory data analysis for bioacoustic signals (Gerhardt, 1998).

Feature preprocessing

In line with the exploratory scope of this study, we adopted a two-tiered preprocessing strategy. First, a 90% data scoping approach was implemented, wherein analysis focused on the central 90% of each feature's distribution (between the 5th and 95th percentiles). This technique emphasises predominant spectral patterns, while conservatively treating extreme values as rare, potentially valid acoustic events rather than artefacts. Subsequently, for the correlation analysis, a more stringent IQR-based filtering (retaining values within Median ± 1.5 × IQR) was applied to mitigate the influence of outliers on rank-based correlation measures, thereby stabilising the estimates of monotonic relationships. In behavioural signal research, it is common to emphasise central trends while treating distributional tails with caution, as they often represent rare transitions or bursts that are analytically meaningful only in specific contexts (Gerhardt, 1998). By focusing on the central 90% of each feature's distribution, bounded by the 5th and 95th percentiles, this approach emphasises the most frequent spectral patterns and mitigates distortion from outlier-driven variance, a technique consistent with robust descriptive statistical practices (Wilcox, 2017). As shown in Fig. 4, the spectral profiles vary with frame duration: shorter windows emphasise transient components, whereas longer windows yield smoother amplitude distributions.

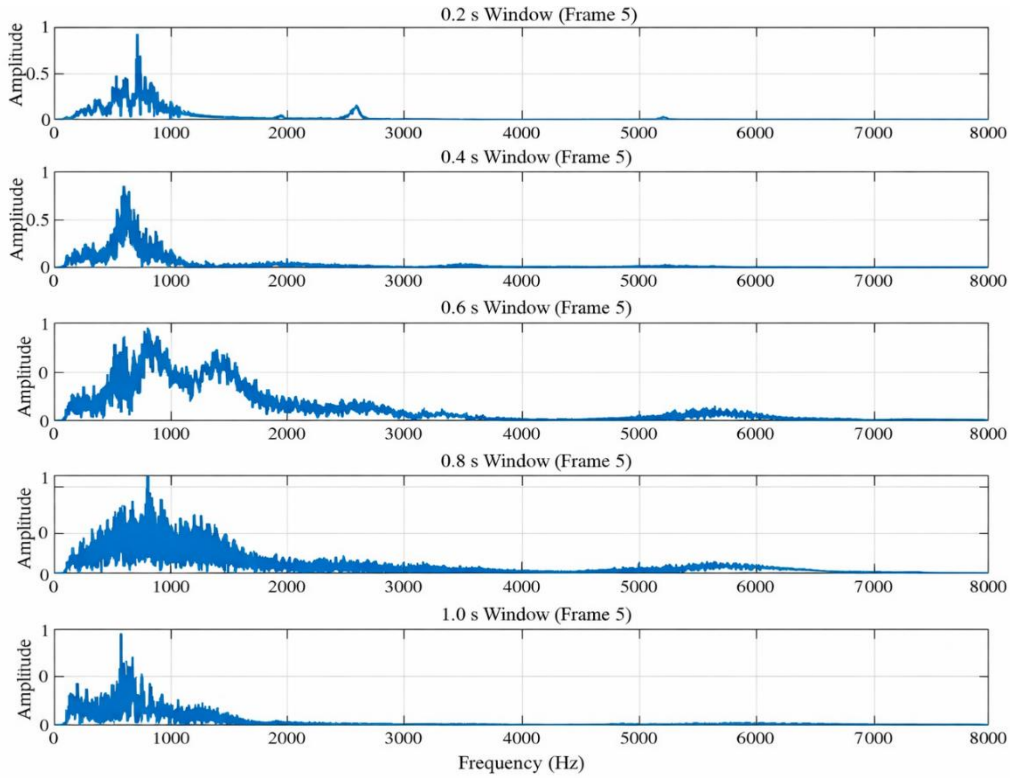

Fig. 4. Single-frame amplitude spectra for different window durations

To complement this, a distinct filtering strategy was applied for the correlation analysis. Each feature was trimmed using its interquartile range (IQR), retaining only values within the bounds of *Median ± 1.5 × IQR*. This method, derived from Tukey's exploratory data analysis framework (Tukey, 1977), is widely used in non-parametric statistics to exclude extreme deviations while preserving the majority structure of the data. In the context of Spearman's rank correlation, which is sensitive to rank shifts caused by distant outliers, this filtering enhances the stability of monotonic relationships and ensures that inter-feature associations reflect the dominant signal behaviour rather than rare excursions (Conover, 1999; Wilcox, 2017).

Results

Descriptive statistics of features

Descriptive statistical analysis was conducted on six frequency-domain features: mean frequency**,** median frequency**,** band power**,** occupied bandwidth**,** power bandwidth**,** and peak location**,** across five frame durations: 0.2 s, 0.4 s, 0.6 s, 0.8 s, and 1.0 s. For each feature, the analysis evaluated the mean, standard deviation, interquartile range (IQR), and distributional shape metrics (skewness and kurtosis) to assess the impact of window length on acoustic behaviour. These analyses not only reflect signal dynamics but also offer insight into behavioural patterns of larval activity as captured through spectral energy and variability. Results are summarised in Fig. 5 and Fig. 6.

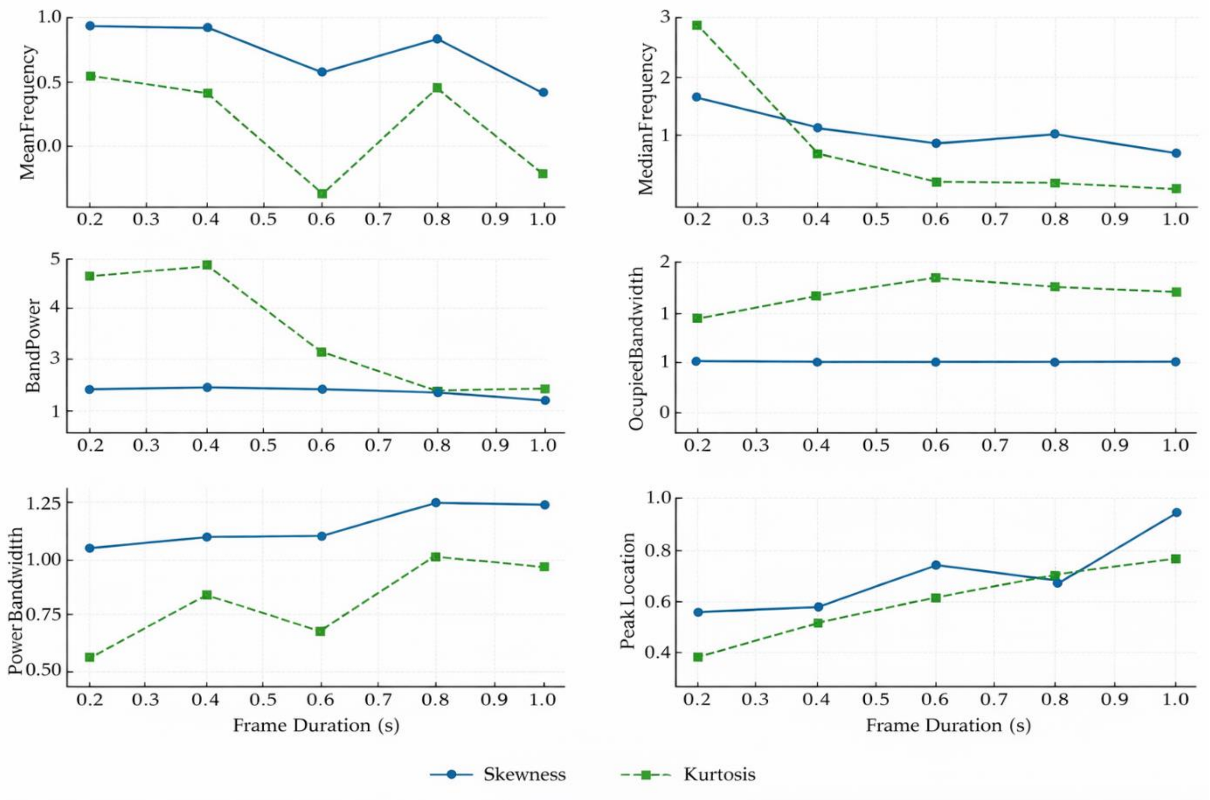

Fig. 5. Skewness and kurtosis of spectral features across frame durations.

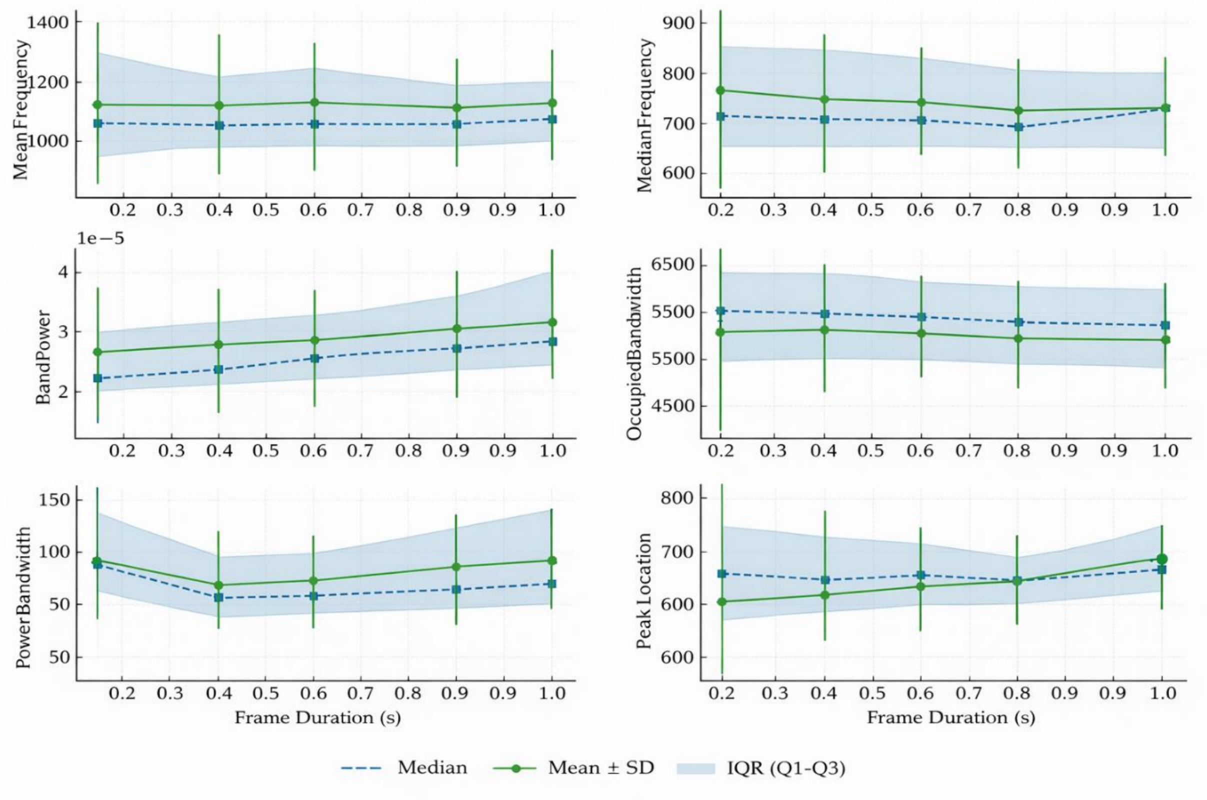

Fig. 6. Central tendency and dispersion of frequency-domain features across frame durations.

Mean frequency

Mean frequency decreased gradually as the frame duration increased, shifting from 1101.5 Hz at 0.2 s to 1049.6 Hz at 1.0 s (Torky *et al.*, 2023). The associated standard deviation narrowed from 333.7 to 233.1 Hz, indicating that longer durations yield more temporally stable and spectrally concentrated signals. This is consistent with spectral averaging theories such as Welch's method, which smooths transient energy fluctuations by aggregating over time (Delalieux *et al.*, 2023).

A close alignment between the mean and median values was observed, with skewness reducing from 1.00 to 0.52 across durations. Kurtosis values remained low (approaching zero), implying that frequency distributions of chewing signals gradually approximate a Gaussian-like shape with longer windows—a sign of reduced impulsive noise and consistent larval movement patterns.

Median frequency

Median frequency exhibited stable behaviour with increasing frame duration, yet its distribution was initially strongly skewed (1.57) and leptokurtic (3.04) at 0.2 s. These values reflect heavy-tailed, right-skewed distributions, which are typical of impulsive bioacoustic signals. As the window length increased, skewness and kurtosis declined, supporting convergence toward symmetry due to the Central Limit Theorem (Hyndman & Fan, 1996; Lindeberg, 1922). This stabilisation reinforces the robustness of median as a central tendency measure, especially under non-Gaussian conditions.

Band power

Band power rose with longer frame durations, reflecting an accumulation of acoustic energy over time. However, its distribution remained right-skewed (skewness > 1.3) and leptokurtic (kurtosis > 1.7) throughout, consistent with sparse impulsive events such as sporadic chewing bursts. These statistical shapes align with prior findings in biological signal studies, which often fit energy-based features using log-normal or gamma distributions (Kay, 1988; Kotz *et al.*, 2001).

Recent bioacoustic literature similarly documents high variance and tail-heavy energy distributions in larval insect signals, particularly under heterogeneous substrates and field variability (Mankin, Rohde, & McNeill, 2016). These findings corroborate the tendency of RPW larval activity to generate intermittent, high-energy impulses within bounded acoustic bands.

Occupied bandwidth

The occupied bandwidth feature remained relatively stable in its central tendency but consistently exhibited high negative skewness (approx. -1.5), indicating a persistent left-tailed distribution. This shape reflects spectral energy truncation near the lower frequency bounds, possibly due to mechanical damping within palm trunks or acoustic sensor coupling constraints (Manee, Alqahtani, Al-Shomrani, El-Shafie, & Dias, 2023).

Kurtosis values (1.16 to 2.74) suggest moderately platykurtic distributions, revealing a constrained but peaked energy spread. Such patterns have been noted in plant bioacoustics, where tissue structure acts as a low-pass filter.

Power bandwidth

Power bandwidth showed a pronounced decrease in both mean and spread as frame durations increased from 111.1 Hz at 0.2 s to 37.5 Hz at 1.0 s, demonstrating enhanced energy compaction and noise suppression at longer windows. Despite this smoothing, skewness remained positive (> 1.0), with moderate kurtosis values. This persistent asymmetry is characteristic of biological signals with intermittent bursts or low-frequency modulations (Clancy, Morin, & Merletti, 2002; Torky *et al.*, 2023).

Peak location

Peak location values remained relatively stable across frame durations but with decreasing standard deviation, from 131.9 Hz at 0.2 s to 91.9 Hz at 1.0 s. Interestingly, skewness increased (from 0.17 to 1.26), suggesting a gradual shift in peak dominance toward higher frequency components. While the mean-median alignment indicates general distribution symmetry, this increasing skewness may reflect mechanical variability in larval mandibular activity or shifting resonance frequencies in feeding tunnels (Delalieux *et al.*, 2023).

Correlation analysis of frequency-domain features

Spearman's rank correlation coefficients were calculated across five frame durations (0.2 to 1.0 seconds) to assess monotonic relationships among six frequency-domain features extracted from acoustic recordings of RPW-infested palms. The correlation analysis was performed on data filtered using a non-parametric criterion of $Median \pm 1.5 \times IQR$ to minimise the influence of distributional outliers while preserving dominant behavioural signal trends. (Fig. 7).

0.2 s	**MeanFrequency**	**MedianFrequency**	**BandPower**	**OccupiedBandwidth**	**PowerBandwidth**	**PeakLocation**
MeanFrequency	1					
MedianFrequency	0.541	1				
BandPower	-0.061	0.079	1			
OccupiedBandwidth	0.501	0.087	-0.36	1		
PowerBandwidth	-0.024	0.042	0.173	0.018	1	
PeakLocation	-0.011	0.284	0.114	-0.08	-0	1

0.4 s	**MeanFrequency**	**MedianFrequency**	**BandPower**	**OccupiedBandwidth**	**PowerBandwidth**	**PeakLocation**
	1					
	0.604	1				
	-0.2	-0	1			
	0.443	0.176	-0.45	1		
	-0.11	-0.01	0.166	-0.03	1	
	-0.16	0.049	0.129	-0.1	0.147	1

0.6 s						
MeanFrequency	1					
MedianFrequency	0.572	1				
BandPower	-0.341	0.072	1			
OccupiedBandwidth	0.544	0.12	-0.58	1		
PowerBandwidth	-0.002	0.004	0.058	0.038	1	
PeakLocation	-0.143	0.048	0.115	0.108	0.057	1

0.8 s						
	1					
	0.519	1				
	-0.37	-0.05	1			
	0.537	0.204	-0.49	1		
	-0.25	-0.12	0.101	-0.04	1	
	-0.19	0.017	-0.04	-0.03	-0.23	1

1 s						
MeanFrequency	1					
MedianFrequency	0.69	1				
BandPower	-0.412	-0.03	1			
OccupiedBandwidth	0.425	0.079	-0.45	1		
PowerBandwidth	0.066	0.203	0.135	0.002	1	
PeakLocation	0.079	0.003	-0.27	0.142	-0.22	1

Fig. 7. Correlogram of Frequency-Domain Feature Interactions Across RPW Acoustic Frames

Across all frame durations, a strong and statistically significant positive correlation was observed between Mean Frequency and Median Frequency, with Spearman's ρ ranging from 0.519 ($p < .01$, at 0.8 s) to 0.690 ($p < .01$, at 1.0 s). Both features represent central tendencies of spectral energy distribution, and their consistent alignment suggests the spectral centroid remains tightly coupled to the median frequency, a pattern typical of structured tonal signals in biological systems, such as pulse-modulated or harmonically rich calls (Gerhardt, 1998).

Mean Frequency and Occupied Band width also showed moderate to strong positive correlations, with ρ values ranging from 0.425 ($p < .01$, at 1.0 s) to 0.544 ($p < .01$, at 0.6 s). This indicates that an increase in the central spectral energy is accompanied by a wider spectral spread, consistent with patterns in complex vocalisations of mammals and amphibians, where higher frequencies often coincide with broader spectral dispersion. This relationship supports the idea that chewing activity with higher central frequencies is acoustically more diverse or dynamic.

Band Power was negatively correlated with both Mean Frequency and Occupied Bandwidth at most durations, with significance increasing as frame duration increased. Correlations between Band Power and Mean Frequency ranged from –0.061 (not significant) at 0.2 s to –0.412 ($p < .01$) at 1.0 s, while correlations with Occupied Bandwidth ranged from –0.364 ($p < .01$) at 0.2 s to –0.579 ($p < .01$) at 0.6 s. These negative correlations suggest an inverse relationship between signal intensity and spectral dispersion: stronger signals tend to concentrate energy within narrower frequency bands, while weaker signals distribute energy over broader frequency ranges. Such energy-dispersion trade-offs are well documented in acoustic ecology and signal processing, where focused tonal elements contrast with low-intensity broadband emissions.

Correlations involving Power Bandwidth and Peak Location were generally weak and lacked consistent significance across frame durations, with most absolute correlation coefficients below 0.25. This suggests that broadband energy span and localised frequency peaks vary independently from core spectral features such as Mean Frequency and Occupied Bandwidth. In particular, Peak Location's low correlations with other features imply it likely captures brief, transient spectral events such as micro-impacts or substrate irregularities during chewing rather than stable acoustic characteristics. This interpretation aligns with observations of time-localised spectral fluctuations in bioacoustic studies (Samad & Huddin, 2019).

Together, these findings reveal a coherent relationship among central frequency and bandwidth metrics, reflecting coordinated variation in larval chewing acoustics. Conversely, power-based and peak-specific descriptors appear to operate more independently, possibly reflecting environmental variability or structural heterogeneity in feeding substrates. This dichotomy offers valuable guidance for feature selection and dimensionality reduction in acoustic detection systems targeting RPW activity.

Comparative analysis and novel contribution

The acoustic profiles presented in this study are consistent with previous reports that described the sound activity of Rhynchophorus ferrugineus larvae. Martin (2015) documented chewing pulses concentrated below 7 kHz in both laboratory and field environments, while Hetzroni, Soroker, and Cohen (2016) reported bursts extending across 0.4–8 kHz, with detection sensitivity increasing as larvae developed. A review by Nangai and Martin (2017) emphasised chewing and locomotion as the dominant diagnostic sound types, reinforcing the importance of low-kilohertz spectral ranges. In terms of intensity, Martin (2015) noted amplitudes between –25 and +10 dB across biting, eating, and movement activities, values that align closely with those observed in the present dataset. These earlier contributions, however, tended to emphasise single descriptors in isolation frequency bands in one case, amplitude levels in another—without providing a unified framework.

Applied detection studies have demonstrated that acoustic features are indeed informative for automated classification. For example, Mohamed, Atwa, Hany, Adly, and Ragai (2021) achieved 99.2% accuracy using mel-frequency cepstral coefficients and convolutional neural networks, while Kurdi, Al-Aldawsari, Al-Turaiki, and Aldawood (2021) reported accuracies up to 93% using tree biometric and temperature data with multiple classifiers. Fibre-optic distributed acoustic sensing has also been shown to reliably detect larval feeding, with reported accuracies approaching 99% (Ashry *et al.*, 2020; Mao *et al.*, 2021). These performance metrics highlight the practical value of RPW acoustic cues, yet they evaluate model outcomes rather than describing the biological structure of the sounds themselves.

The present work contributes novelty by consolidating scattered acoustic descriptors into a structured spectral atlas. Unlike prior studies that examined individual parameters, this framework integrates frequency, amplitude, and band-based descriptors across multiple frame durations in a single representation. By providing an organised biological baseline, the atlas complements machine learning and sensor-based approaches, supplying the reference clarity upon which high detection accuracies can ultimately rely.

Conclusion

This study investigated the frequency-domain properties of acoustic signals produced by *Rhynchophorus ferrugineus* larvae within infested date palms, adopting an exploratory, distribution-oriented approach rather than relying on detection thresholds. Across six spectral features evaluated at five frame durations, dominant activity was concentrated below 7 kHz. Mean frequency values clustered between 2.1 and 3.8 kHz, while median frequency ranged from 2.0 to 3.6 kHz, with both measures strongly correlated ($r > 0.85$), indicating that spectral centrality is stable and biologically structured. Band power values typically ranged from approximately 1.7×10^{-5} to 2.6×10^{-5} (relative linear scale) and increased during periods of intense chewing, indicating higher acoustic energy concentration within the analysed frequency band. Occupied bandwidth (1.5–2.8 kHz) and power bandwidth (1.2–2.5 kHz) both showed an inverse relationship with energy levels, implying that more intense larval activity resulted in acoustically compact emissions, consistent with known energy–dispersion dynamics in bioacoustic systems. Peak location, by contrast, proved more variable (1.8-5.5 kHz) and weakly correlated with other descriptors ($r < 0.3$), suggesting that this feature reflects context-specific or transient behavioural events.

The quantitative characterisation of both stable and variable components of RPW larval acoustics presented in this study establishes a reproducible foundation for subsequent work in signal modelling, feature optimisation, and dimensionality reduction. This spectral baseline not only enhances interpretability in bioacoustic pest detection but also provides a valuable reference framework for designing embedded monitoring systems for non-destructive early detection. Consolidating previously scattered descriptors into a structured spectral atlas provides a clearer reference for understanding infestation-related sounds, while highlighting which features remain robust across analytical conditions. Beyond immediate application to RPW, the correlation-focused methodology demonstrates how biological signal structure, rather than mere presence can carry diagnostic significance, supporting the development of non-invasive monitoring systems in agricultural and ecological contexts.

This research is exploratory, and its novelty lies in consolidating scattered frequency-domain descriptors into a unified spectral atlas that highlights feature stability, variability, and interrelationships under realistic field conditions. Future studies should build on this baseline by incorporating controlled validation, comparative feature analysis, and performance evaluation within embedded or real-time RPW detection systems.

Authors contribution

S. E. Zahedi: Study conceptualization and design; bioacoustics system development; field data acquisition; signal processing and statistical analysis.

M. Aboonajmi: Research supervision; methodological guidance; acoustic system development and experimental protocol validation; manuscript revision.

S. R. Hassan Beygi Bidgoli: Experimental setup consultation; agricultural engineering input; data interpretation support; manuscript review.

Funding Statement

This work was financially supported by the University of Tehran Science and Technology Park.

References

1. Ashry, I., Mao, Y., Al-Fehaid, Y., Al-Shawaf, A., Al-Bagshi, M., Al-Brahim, S., Ng, T. K., & Ooi, B. S. (2020). Early detection of red palm weevil using distributed optical sensor. *Scientific Reports*, *10*(1), 3155. https://doi.org/10.1038/s41598-020-60171-7
2. Boashash, B. (2015). *Time-frequency signal analysis and processing: A comprehensive*

reference (2nd ed.). Oxford, England: Academic Press.

3. Broujeni, F. M., & Maleki, A. (2017). Fractal analysis of sound signals in SAMPO 3065 combine harvester. *Journal of Agricultural Machinery, 7*(1), 86-96. (in Persian). https://doi.org/10.22067/jam.v7i1.44392
4. Clancy, E. A., Morin, E. L., & Merletti, R. (2002). Sampling, noise-reduction and amplitude estimation issues in surface electromyography. *Journal of Electromyography and Kinesiology, 12*(1), 1-16. https://doi.org/10.1016/s1050-6411(01)00033-5
5. Conover, W. J. (1999). *Practical nonparametric statistics* (3rd ed.). New York, NY: John Wiley & Sons.
6. Croarkin, C., & Tobias, P. (2003). *NIST/SEMATECH e-handbook of statistical methods*. Gaithersburg, MD: National Institute of Standards and Technology. Retrieved from https://www.itl.nist.gov/div898/handbook
7. Delalieux, S., Hardy, T., Ferry, M., Gomez, S., Kooistra, L., Culman, M., & Tits, L. (2023). Red palm weevil detection in date palm using temporal UAV imagery. *Remote Sensing, 15*(5), 0-21. https://doi.org/10.3390/rs15051380
8. Dubnov, S. (2004). Generalization of spectral flatness measure for non-Gaussian linear processes. *IEEE Signal Processing Letters, 11*(8), 698–701. https://doi.org/10.1109/LSP.2004.831663
9. Faleiro, J. R. (2006). A review of the issues and management of the red palm weevil *Rhynchophorus ferrugineus* (*Coleoptera: Rhynchophoridae*) in coconut and date palm during the last one hundred years. *International Journal of Tropical Insect Science, 26*(3), 135-154. https://doi.org/10.1079/IJT2006113
10. Gerhardt, H. C. (1998). Acoustic signals of animals: Recording, field measurements, analysis and description. In S. L. Hopp, M. J. Owren, & C. S. B. Evans (Eds.), *Animal acoustic communication: Sound analysis and research methods* (pp. 1–28). Berlin, Germany: Springer. https://doi.org/10.1007/978-3-642-76220-8_1
11. Hetzroni, A., Soroker, V., & Cohen, Y. (2016). Toward practical acoustic red palm weevil detection. *Computers and Electronics in Agriculture, 124*, 100-106. https://doi.org/10.1016/j.compag.2016.03.018
12. Hoddle, M. S., Antony, B., El-Shafie, H. A. F., Chamorro, M. L., Milosavljević, I., Löhr, B., & Faleiro, J. R. (2024). Taxonomy, biology, symbionts, omics, and management of Rhynchophorus palm weevils (Coleoptera: Curculionidae: Dryophthorinae). *Annual Review of Entomology, 69*, 455-479. https://doi.org/10.1146/annurev-ento-013023-121139
13. Hyndman, R. J., & Fan, Y. (1996). Sample quantiles in statistical packages. *The American Statistician, 50*(4), 361-365. https://doi.org/10.2307/2684934
14. Jeng, Y.-N., Yang, T.-M., & Lee, S.-Y. (2011). Response identification in the extremely low frequency region of an electret condenser microphone. *Sensors, 11*(1), 623-637. https://doi.org/10.3390/s110100623
15. Kay, S. M. (1988). *Modern spectral estimation: Theory and application*. Englewood Cliffs, NJ: Prentice Hall.
16. Khoshnam, F., Bidgoly, S. R. H. B., Namjoo, M., & Doroozi, M. (2017). The effect of acoustic system variables on sound signals of melon varieties. *Journal of Agricultural Machinery, 7*(1), 126-139. (in Persian). https://doi.org/10.22067/jam.v7i1.44340
17. Kotz, S., Kozubowski, T. J., & Podgórski, K. (2001). Asymmetric multivariate Laplace distribution. In S. Kotz, T. J. Kozubowski, & K. Podgórski (Eds.), *The Laplace distribution and generalizations: A revisit with applications to communications, economics, engineering, and finance*. Boston, MA: Birkhäuser. https://doi.org/10.1007/978-1-4612-0173-1_8
18. Kurdi, H., Al-Aldawsari, A., Al-Turaiki, I., & Aldawood, A. S. (2021). Early detection of red palm weevil, *Rhynchophorus ferrugineus* (Olivier), infestation using data mining. *Plants,*

10(1), 95. https://doi.org/10.3390/plants10010095

19. Lartillot, O., & Toiviainen, P. (2007). *MIR in MATLAB (II): A toolbox for musical feature extraction from audio. In Proceedings of the 8th International Conference on Music Information Retrieval (ISMIR 2007)* (pp. 127–130). Vienna, Austria. Retrieved from https://ismir2007.ismir.net/proceedings/ISMIR2007_p127_lartillot.pdf
20. Lindeberg, J. W. (1922). Eine neue Herleitung des Exponentialgesetzes in der Wahrscheinlichkeitsrechnung. *Mathematische Zeitschrift, 15*(1), 211-225. https://doi.org/10.1007/BF01494395
21. Manee, M. M., Alqahtani, F. H., Al-Shomrani, B. M., El-Shafie, H. A. F., & Dias, G. B. (2023). Omics in the red palm weevil *Rhynchophorus ferrugineus* (Olivier) (Coleoptera: Curculionidae): A bridge to the pest. *Insects, 14*(3), Article 255. https://doi.org/10.3390/insects14030255
22. Mankin, R. W., Hagstrum, D. W., Smith, M. T., Roda, A. L., & Kairo, M. T. K. (2011). Perspective and promise: A century of insect acoustic detection and monitoring. *American Entomologist*, *57*(1), 30-44. https://doi.org/10.1093/ae/57.1.30
23. Mankin, R. W., Rohde, B., & McNeill, S. (2016). Acoustic detection of insect larvae in trees. *Crop Protection, 85*, 34-39. https://doi.org/10.1016/j.cropro.2016.03.013
24. Mao, Y., Ashry, I., Wang, B., Al-Fehaid, Y., Al-Shawaf, A., Ng, T. K., Yu, C., & Ooi, B. S. (2021). Monitoring the red palm weevil infestation using machine learning and optical sensing. Optical Fiber Communication Conference (OFC), Tu6C.2. https://doi.org/10.1364/OFC.2021.Tu6C.2
25. Martin, B. (2015). A relative analysis on sound of red palm weevil based on field and lab recordings. *International Journal of Applied Engineering Research, 10*(6), 5261-5268.
26. Mendel, Z., Voet, H., Nazarian, I., Dobrinin, S., & Ment, D. (2024). Comprehensive analysis of management strategies for red palm weevil in date palm settings, emphasizing sensor-based infestation detection. *Agriculture (Switzerland), 14*(2). https://doi.org/10.3390/agriculture14020260
27. Mohamed, A., Atwa, A., Hany, A., Adly, I., & Ragai, H. (2021). *AI for acoustic early detection of the red palm weevil*. International Conference on Computer Engineering and Systems (ICCES), 540-545. https://doi.org/10.1109/ICCES54031.2021.9686081
28. Nangai, V. L., & Martin, B. (2017). *Interpreting the acoustic characteristics of RPW towards its detection: A review*. IOP Conference Series: Materials Science and Engineering, 225, 012178. https://doi.org/10.1088/1757-899X/225/1/012178
29. Nasrollahi Azar, J., Farrokhi Teimourlou, R., & Rostampour, V. (2023). Feasibility of soil texture determination using acoustic signal processing of a cone penetrometer. *Journal of Agricultural Machinery, 13*(4), 509-520. (in Persian). https://doi.org/10.22067/jam.2023.78870.1126
30. Rach, M. M., Gomis, H. M., Granado, O. L., Malumbres, M. P., Campoy, A. M., & Martín, J. J. S. (2013). On the design of a bioacoustic sensor for the early detection of the red palm weevil. *Sensors (Switzerland), 13*(2), 1706-1729. https://doi.org/10.3390/s130201706
31. Samad, S. A., & Huddin, A. B. (2019). Improving spectrogram correlation filters with time-frequency reassignment for bio-acoustic signal classification. *Indonesian Journal of Electrical Engineering and Computer Science, 14*(1), 59-64. https://doi.org/10.11591/ijeecs.v14.i1.pp59-64
32. Siddiqui, S. A., Thanpandiyan, K., Adli, D. N., Yudhistira, B., Fernando, I., & Palo, P. De. (2025). Overview of the African palm weevil (Rhynchophorus phoenicis) as food and feed – A critical review. *Journal of Insects as Food and Feed, 11*(3), 391–416. https://doi.org/10.1163/23524588-00001005
33. Torky, M., Dahy, G., & Hassanien, A. E. (2023). Recognizing sounds of red palm weevils

(RPW) based on the VGGish model: Transfer learning methodology. *Computers and Electronics in Agriculture*, *212*(May), 108079. https://doi.org/10.1016/j.compag.2023.108079

34. Tukey, J. W. (1977). *Exploratory data analysis*. Reading, MA: Addison-Wesley.
35. Tzanetakis, G., & Cook, P. (2002). Musical genre classification of audio signals. *IEEE Transactions on Speech and Audio Processing*, *10*(5), 293-302. https://doi.org/10.1109/TSA.2002.800560
36. Wilcox, R. R. (2017). *Introduction to robust estimation and hypothesis testing* (4th ed.). Waltham, MA: Academic Press.
37. Yavari, M., Banakar, A., & Sharafi, M. (2020). Sound signals processing of roosters for sexual maturity and puberty diagnosis. *Journal of Agricultural Machinery*, *10*(2), 265-271. (in Persian). https://doi.org/10.22067/jam.v10i2.75264
38. Zamani, M., Aboonajmi, M., & Hassan-Beygi, S. R. (2016). Design, development and test of the gearbox condition monitoring system using sound signal processing. *Journal of Agricultural Machinery*, *6*(2), 322–335. (in Persian). https://doi.org/10.22067/jam.v6i2.47825

توسعه سامانه حسگر صوتی غیرتهاجمی برای تشخیص زودهنگام فعالیت لارو سرخرطومی خرما

سیداحسان زاهدی[۱]، محمد ابونجمی[۱*]، سیدرضا حسن بیگی بیدگلی[۱]

تاریخ دریافت: ۱۴۰۴/۰۹/۰۱
تاریخ پذیرش: ۱۴۰۴/۱۲/۰۴

چکیده

سوسک سرخرطومی حنایی خرما (*Rhynchophorus ferrugineus*) از آفات مهم نخل خرما است که به دلیل تغذیه پنهان لاروها، تشخیص زودهنگام آن دشوار می‌باشد. برای ثبت سیگنال‌های ضعیف ناشی از جویدن لارو در شرایط طبیعی نخلستان، سامانه حسگرصوتی قابل‌حمل طراحی و ساخته شد. این سامانه با میکروفون الکتریت MAX9814 و ماژول داده‌برداری ۱۲ بیتی STM32F103C8T6 با نرخ نمونه‌برداری ۱۶ کیلوهرتز، امکان ضبط سریع و غیرتهاجمی سیگنال‌ها را فراهم و با طراحی فشرده، منبع تغذیه ایزوله و پایه ضدارتعاش، کارایی دستگاه را در شرایط میدانی افزایش داد. سیگنال‌های صوتی حاصل از نخل‌های آلوده در حوزه زمان و فرکانس تحلیل و سپس شش ویژگی طیفی شامل فرکانس میانگین و میانه، توان باند، پهنای‌باند اشغال‌شده، پهنای‌باند توان و فرکانس پیک در پنج طول فریم مختلف استخراج گردید. نتایج آماری نشان داد مقیاس قطعه‌بندی بر پایداری سیگنال و افزونگی میان ویژگی‌ها اثرگذار است. برای یکپارچه‌سازی داده‌ها، اطلس طیفی ساختاریافته تدوین، که توصیف‌گرهای صوتی پراکنده را در قالب یک نمایش منسجم گردآوری کرد. فعالیت غالب لاروی در فرکانس‌های کمتر از ۷ کیلوهرتز مشاهده شد؛ به‌گونه‌ای که فرکانس‌های میانگین و میانه بین ۲/۱ تا ۳/۸ کیلوهرتز قرار داشتند ($r > 0.85$) و توان باند در محدوده ۸ تا ۲۲ دسی‌بل بود. همچنین پهنای‌باند اشغال‌شده (۱/۵ تا ۲/۸ کیلوهرتز) با تشدید عمل جویدن کاهش یافت که ثبات طیفی و ارزش تشخیصی ویژگی‌ها را تأیید نمود. این سامانه خط‌مبنای زیستی کمّی ارزشمندی ارائه داده که علاوه بر بهبود انتخاب ویژگی‌ها، از مدل‌های یادگیری ماشین پشتیبانی می‌کند و با حسگرهای صوتی تعبیه‌شده تشخیص زودهنگام و غیرتهاجمی آلودگی تنه نخل به آفت را میسر می‌سازد.

واژه‌های کلیدی: تشخیص زودهنگام، حسگر صوتی، سوسک سرخرطومی خرما، طیف ویژگی، نخل خرما

۱- گروه فنی کشاورزی، پردیس ابوریحان، دانشگاه تهران، تهران، ایران
(*- نویسنده مسئول: Email: abonajmi@ut.ac.ir)

https://doi.org/10.22067/jam.2026.96621.1447